The Pennsylvania State University

Wind Energy Club

Technical Design Report

Submitted to the 2022 U.S. Department of Energy Collegiate Wind Competition

April 24, 2022

Aerodynamics

Joshua Bannon	**Lead**
Brittany Nelson	Member
Victor Yang	Member
Allison Karp	Member
Jason Oh	Member
Shana Hartwick	Member
Jaynum V. Patel	Member
Sebastian Caballero	Member
Mario Banci	Member

Generator & Structures

Eric Sarbacker	**Co-Lead, President**
Eric Folmar	**Co-Lead**
Zoe Shu	Foundation lead
Nick Bowers	Member
Massimo Finx	Member

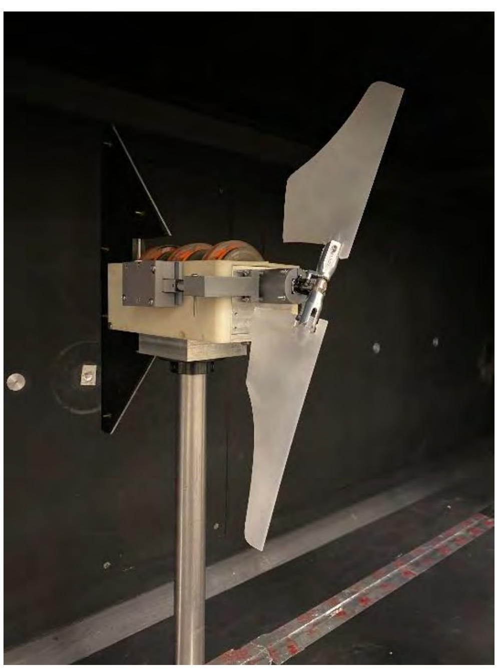

Electronics & Software

Satyam Patel	**Lead, Vice-President**
James Leandri	Software Director
Conner Burger	Control B. Director
Anum Jan	Buck B. Director
Jackie Cheng	Load B. Director
Tara Presnall	Systems I. Director
Brian Truong	Member
Rahul Shekar	Member
Andrew Rednikov	Member
Fola Omogboyega	Member
Lily McGinnis	Member
Haiden Shober	Member
Dominic Touma	Member
Max Zingman	Member
Hamdan Almarzooqi	Member

Academic Advisors

Dr. Mark Miller	**Test Turbine**
Dr. Susan Stewart	Project Development
Dr. Yan Li	Electronics Advisor
Mr. Richard Auhl	System Testing
Dr. Sven Schmitz	Advisor

Table of Contents

Executive Summary 3
1.0.0 Aerodynamics & Rotor 3
1.1.0 Rotor Implementation & Introduction 3
1.2.0 Blade Strength Testing 5
1.3.0 Blade Pitch Mechanism 6
2.0.0 Generator & Structures 7
2.1.0 Generator 7
3.0.0 Foundation 9
3.1.0 Suction Caisson Design 9
3.2.0 Caisson Model Testing 9
4.0.0 Electronics & Software 10
4.1.0 Control States & Safety Tasks 11
4.1.1 Start-Up 11
4.1.2 Optimization Region I 12
4.1.4 Optimization Region II 12
4.1.5 Abnormal Override 13
4.1.6 Shutdown Sequence 13
4.2.0 Control Circuit 14
4.3.0 Safety Buck System 14
4.4.0 Variable Load System 16
4.5.0 Software 16
5.0.0 Turbine Testing 16
5.1.0 Power Curve Performance 16
5.2.0 Safety & Restart Task 19
5.3.0 Durability Task 19
5.4.0 Commissioning Checklist 19
5.5.0 Conclusion 21
Appendix A. Overall Design Choices 21
References i

Executive Summary

Offshore wind energy projects have great potential to provide clean and reliable energy. In this report, The Pennsylvania State University Wind Energy Club will introduce the design of a scale, offshore, fixed-bottom wind turbine. The design of this turbine has been divided into three primary subsystems: aerodynamics, generator & structures, and electronics & software. The paramount objective of the team was to design a well optimized aerodynamic, mechanical, and electrical system. The team emphasized three values when engineering the turbine: performance, reliability, and safety.

Regarding the aerodynamics and rotor system, the team has worked on implementing a new pitching mechanism that relies on two linear servos, rather than the single radial servo as in previous years. The choice of airfoil, chord distribution, and twist distribution remains unchanged this year, but the quality of the 3D printed blades being used for wind tunnel testing has improved. Last year, the blades were less stiff than the team had hoped, and large sections of the blade were incredibly tessellated. New blades were printed at the end of the 2021 competition year, but not enough time remained to allow for comprehensive wind tunnel testing. This year, those new and improved blade prints have been wind tunnel tested thoroughly as has the newly modified pitching system. The blades have also been strength tested with the new material.

Our teams axial flux generator design has been used for its better startup and overall performance over radial or vertical axis designs. To accompany the new challenge of building an offshore wind turbine foundation, our subteam mainly focused on that topic; but thorough data was collected on our dynamometer stand to see if our hypothesis of active stage variation could help prevent our turbine from producing dangerously high voltage. With thoughtful attention to the competition, the design of our foundation was founded in research of current designs and understanding of areas of failure.

Following previous competitions, the team has totally redesigned the electronics system. The team has significantly increased focus on the software design. With the addition of four new sensors, the team has had much greater control over each aspect of the system. For instance, the accelerometer is used to detect a topple of the turbine, and in doing so, try to correct the topple by inducing a reverse torque by changing blade pitch. In addition, the team transitioned from using a constant load to a variable load, enabling maximum power point tracking. New and efficient rectification and regulation circuits have been implemented. In previous years, the team has failed all attempts to implement a buck circuit. The team was finally successful in implementing a switching buck circuit that limits PCC voltage to 48V while maximizing power production.

1.0.0 Aerodynamics & Rotor

1.1.0 Rotor Implementation & Introduction

The team this year has been focused on optimizing the two-bladed rotor design that was envisioned for the 2021 competition year in order to achieve the improvements in power coefficient that are seen in Figure 1.1. Therefore, no additional design work on the blades was completed this year, but a brief explanation of the design process has been included. Little wind tunnel testing was completed last year due to time and wind tunnel availability constraints, but the team has been much more successful in performing testing this year. To add, the newest 3D print of the blades was strength tested using purpose-made clamps designed to fit the chord, airfoil, and twist of the blade at different radial lengths, and one blade was strength tested until failure.

New to this year is the 3D printing and implementation of a revised pitching mechanism. This mechanism relies on two linear servos, rather than the single radial servo from prior years. The goal with this change was to produce a more reliable and consistent pitch mechanism. While this system is more complex than the previous version, there have been no major issues with the mechanism during testing that weren't easily resolved.

Initially, the aerodynamics sub-team also planned to redesign the nacelle to improve aerodynamics and ease-of-use, but time constraints and the need to complete the pitch mechanism and wind tunnel testing became too pressing. As such, a possible goal for the 2023 competition could be to redesign the nacelle.

Figure 1.1: Cp vs TSR, PSU CWC 2019 Rotor, 3 vs 2 Blades

Equation 1[1] below was used last year as a guide when producing the chord distribution for the two-bladed rotor. This equation produces the optimal chord distribution for a rotor given blade number *B*, tip speed ratio λ, lift coefficient C_l, and chord relation c(r/R).

$$B\lambda c_l * c\left(\frac{r}{R}\right) = \left(\frac{4}{3}\right)^2 \pi \frac{1}{\lambda_r} \qquad (1)$$

(a)

(b)

(c)

Figure 1.2: Blade 3D Print Evolution

For a more reasonable and practical shape, chord lengths towards the root of the blade were decreased. XTURB[2], a Blade Element Momentum Theory code developed at Penn State, was used to analyze the blade shape and twist, and changes were made iteratively to determine optimal characteristics. The results are detailed further in a C_P vs λ graph shown in the Turbine Testing Section 5.1.0 that is compared with experimental data. Once chord distribution and twist were finalized, the MA 409 airfoil was imported to SolidWorks and the shape was repeated across 52 planes while being adjusted for the predetermined chord and twist values. This blade file was sent for 3D-printing to a third-party company, using Nylon 12 as the material. Among others, this print is shown in Figure 1.2a. However, upon receiving this first print, the blades were tessellated, and the tip deflection was extreme due to a lack of stiffness. These problems were resolved with a second print in a new material, Accura 60. This second set of the blades has been used extensively for wind tunnel and strength testing, and as such, the thinner trailing edges are slightly cracked and chipped. Therefore, the decision was made to order a third set of blades for ideal turbine performance without cracked or chipped blades; this will also allow for stress testing to failure for one blade, something that has yet to be done for this rotor. The full evolution of the blade prints is shown in Figure 1.2.

1.2.0 Blade Strength Testing

To test the blade strength, our team designed three clamps in SolidWorks, and these clamps were later 3D printed. Figure 1.3 depicts the configuration of the clamps: one near the root, one at the midspan, and one near the tip. At a blade radius of 1.34 inches (the clamp location nearest the hub), our team applied up to 33.75 ounces to the clamp using a hook and 16oz iron weights shown in Figure 1.4. No noticeable blade deflection was seen. At a blade radius of 3.68 in. (the midspan), deflection was increasingly seen across the blade as more weight was added. The 2nd lightest weight of 9.75 oz. resulted in a deflection of 0.05 in. at the clamp and 0.158 in. at the tip. The heaviest weight of 33.75 oz. resulted in a deflection of 0.2 in. at the clamp and 0.3955 in. at the tip. As expected, much more deflection was seen for forces applied to the tip clamp. At a blade radius of 7.1 in., the lightest weight of 1.75 oz. resulted in a deflection of 0.09 in., and the heaviest weight of 33.75 oz. displayed a deflection of 0.95 in. To add, the team tested one blade to failure, and the blade reached 110 ounces before breaking. Notably, testing the Accura 60 blades was new for 2022 as we were unable to complete these tests for the 2021 competition.

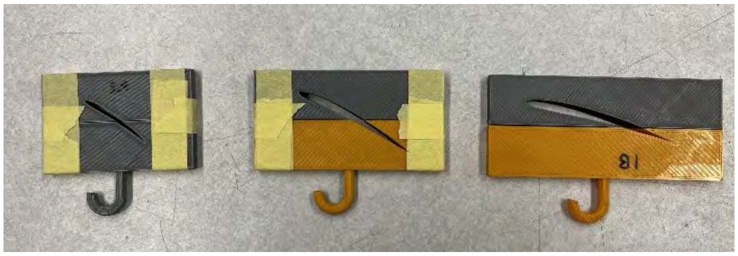

Figure 1.3: Strength Test Clamps

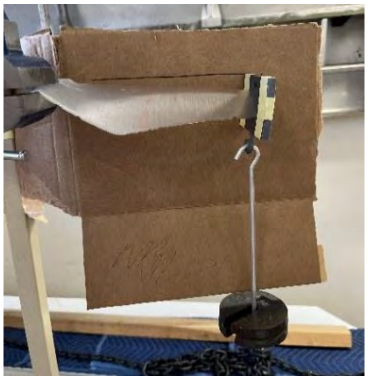
Figure 1.4: Tip Deflection with 33.75 Ounces Load

Table 1.1: Blade Stress Test Data

Weight (oz.)	Deflection for Clamp at 1.34 inches (in.)	Midspan Deflection for Clamp at 3.68 inches (in.)	Tip Deflection for Clamp at 3.68 inches (in.)	Deflection for Clamp at 7.1 inches (in.)
1.75	0	0	0	0.09
9.75	0	0.05	0.158	0.31
17.75	0	0.076	0.218	0.52
25.75	0	0.13	0.3055	0.78
33.75	0	0.2	0.3955	0.95

Comparing these results with expected aerodynamic forces, the predicted maximum thrust force generated by the turbine is 11.41 pounds, or 182.56 ounces. This is for a maximum thrust coefficient C_T of 0.83 and wind speed of 25 m/s. While this force is more than the blades' maximum strength of 110 ounces, no significant tip deflection has been observed during wind tunnel testing, even at speeds of 25 m/s. As such, concerns about blade failure due to high thrust and dip deflection are minimal.

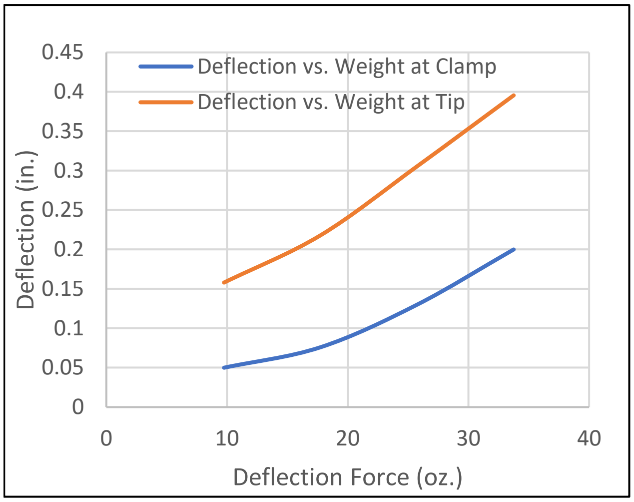

Figure 1.5: Deflection vs Deflection Force at Blade Radius of 3.68 in.

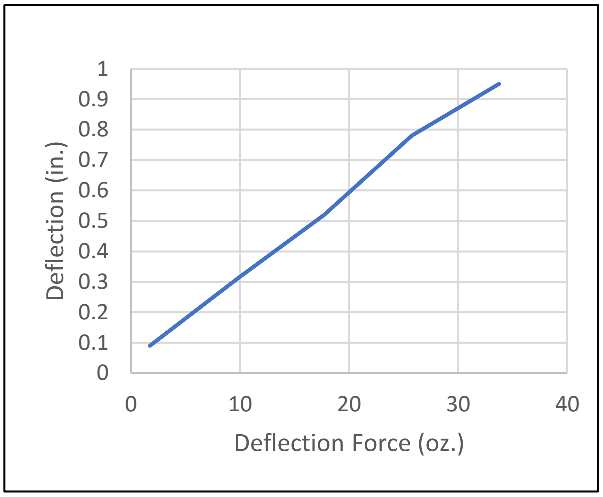

Figure 1.6: Deflection vs. Deflection Force at a Blade Radius of 7.1 in.

1.3.0 Blade Pitch Mechanism

The blade pitch mechanism is designed to adjust the pitch of the blades. The mechanism is composed of mostly 3D printed components and two linear servos. The linear servos are positioned on the sides of the nacelle and connected to the rotor hub by two arms. Initial testing of the mechanism found that the blades would collide with the arms resulting in a narrow range of pitch angles for the blades. To increase the range of motion for the blades, either the blades needed to have areas removed or the rotor hub would need to be moved further away from the point of contact. The latter option was chosen to avoid modifying the blade shape, and the results are shown in Figure 1.7. The circular hub pieces that attached the pitch mechanism to the main assembly were extended, moving the bracket arms closer to the nacelle. Testing with this new design showed that while the arms were no longer in the path of the blades, retracting the linear servos would now cause the arms to contact the nacelle. The initial angled design of the bracket arms was replaced with a design that connected to the circular hub at a 90° angle, finally allowing the servos to move through their full necessary range. The results of this change are shown in Figure 1.8. Additionally, the initial construction of the pitch mechanism is shown in Figure 1.9.

Figure 1.9: First-Pass Assembly of the Pitch Mechanism Prior to Revisions

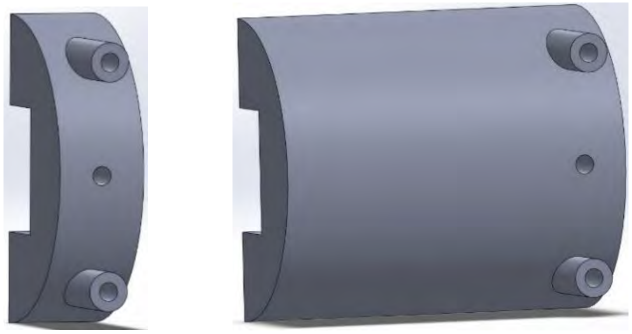

(a) (b)

Figure 1.7: Rotor Hub Clamp Before (a) and After (b) Revision

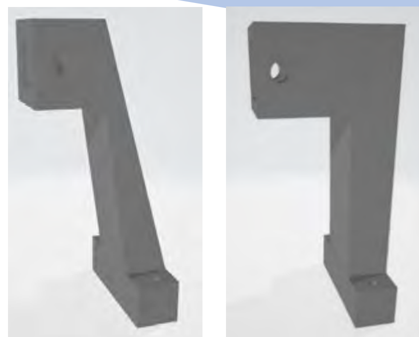

(a) (b)

Figure 1.8: Bracket Arm Design Before (a) and After (b) Revision

2.0.0 Generator & Structures

2.1.0 Generator

For the 2022 Competition, the team used the same generator as the prior year, instead focusing on improving the overall performance and exploring a novel method for shifting the generator power curve called Active Stage Variation. One issue that became apparent during early testing of our generator was that each of its three stages was producing different voltages at a given rotational speed. Through testing several variables one at a time, it was determined that the cause for these voltage discrepancies was inconsistency in the air gaps between the rotors and stators. To solve this problem, rotor spacers were designed in SolidWorks and 3D-printed. The design and application of these spacers can be seen in Figures 2.1 and 2.2. Through the utilization of these spacers to ensure the consistency of the air gaps, the voltage discrepancies were virtually eliminated, as can be seen in Figure 2.3.

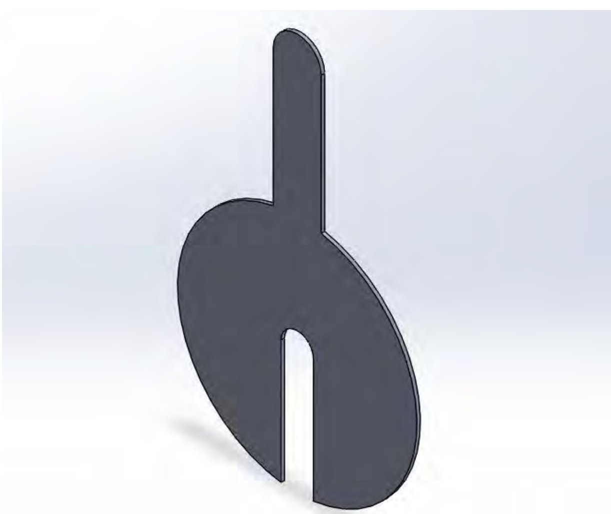

Figure 2.1: SolidWorks Model of Rotor Spacer

Figure 2.2: Application of Rotor Spacers

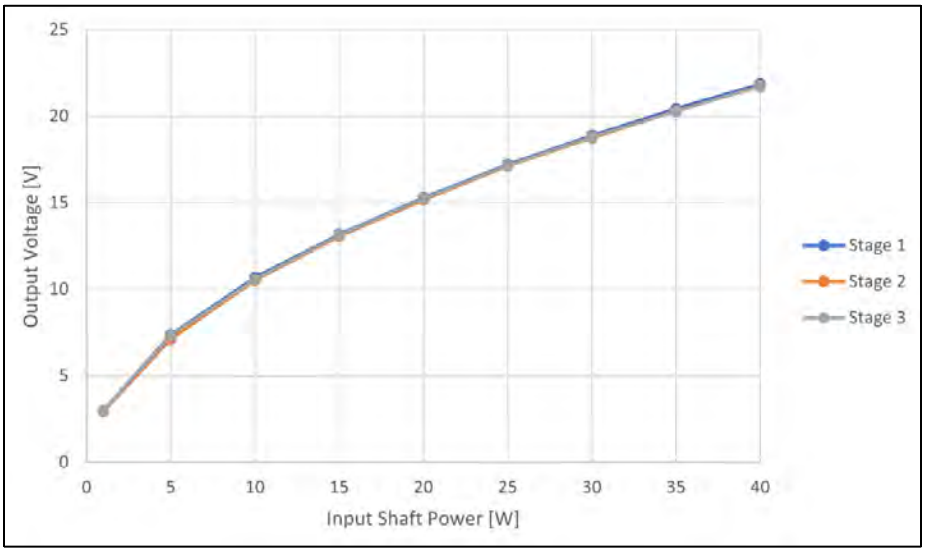

Figure 2.3: Individual Stage Voltage vs. Shaft Power Comparison (20 Ω Generator Load)

Our concept for Active Stage Variation was tested on the dynamometer test stand using a circuit that allowed the connection of each stage to the load to be controlled independently. It was found that this technique allows for control over the generator's power-RPM curve in a manner similar to load variation, as can be seen in Figure 2.4[3]. While not implemented in our 2022 Competition turbine, Active Stage Variation could prove useful in future years when combined with active load variation, especially at lower wind speeds.

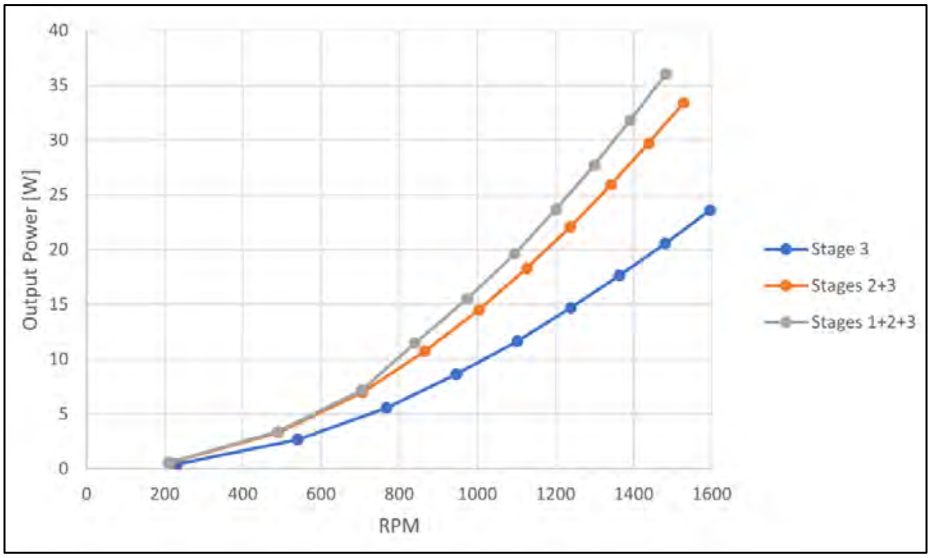

Figure 2.4: Variable Stage Output Power vs. Rotational Speed Comparison (20 Ω Generator Load)

3.0.0 Foundation

3.1.0 Suction Caisson Design

The addition of the offshore component in the competition requires the integration of a brand-new subsystem that is critical to the operation of the turbine. For this reason, a new subteam was formed to research and produce the foundation piece.

Initial research of current offshore designs revealed a wide array of possible designs ranging from complex towers to simple monopoles. From the literature[1], it was found that the common part used in almost all foundations is a suction caisson. A suction caisson has an incredibly straightforward design that would suit the competition challenges well. The necessity of having a completely ferrous foundation makes it difficult to produce a complex design as parts that require welding, machining, or even tools for installation that are either expensive or difficult to work with. A monopole suction caisson design was favorable because it has the simplest design, but it is still incredibly customizable in its shape. All that would be required is a plate to be welded to a pipe and attached to a flange, then a small hole for a check valve (Figure 3.1).

Figure 3.1: Checking vacuum seal of a model

3.2.0 Caisson Model Testing

Due to financial constraints, 3D printed caissons were used to determine the optimal sizing for our foundation. From the literature, it was determined that the main point of failure would be due to caisson rotation[4,5], as most other points of failure are due to the long-term deterioration from the ocean[1]. The literature focused on vertical and horizontal loading, frequency induced stresses, bearing capacity, and limit states, rather than analytical methods of determining tip-over moments on a suction caisson. To overcome this, our team decided to conduct a test in order to determine the optimal suction caisson geometry for the competition turbine. Six test foundations were 3D printed, changing the diameter, length, and skirt thickness to determine how each variable affected the maximum tip-over moment that the foundation could withstand. The test foundations are made of PLA material and were connected to a simple flange-vacuum system (Figure 3.2) to determine tip over moment.

Figure 3.2: Model Caisson Testing Set-up

The results of our testing (Table 3.1) indicated that the maximum moment that the foundation can manage is directly proportional to the interior volume of the caisson. With the help of the aero team, we determined that the maximum thrust force our turbine would experience in the strength test was 50.1 N, leading to an overall moment of 28.3 Nm. To resist this moment (plus an extra 50% safety factor) the estimated volume required would be 760 in^4, or a length of 12 in and a diameter of 9 in – to fit within competition guidelines. A competition foundation has not yet been built due to the prohibitive cost of a large diameter steel pipe, which will be resolved by using a rolled steel section instead.

Table 3.1: Model Caisson Data

Diameter (in.)	Length (in.)	Thickness (in.)	Internal Volume (in^3)	Tip over force (lbs.)	Max Moment (Nm)
2	4	1/4	12.57	1	1.07
2	4	1/8	12.57	1	1.07
3	4	1/8	28.27	1.25	1.41
4	2	1/8	25.13	0.5	0.54
4	6	1/8	75.4	4	4.07
9	12	1/8	763.41	< 11.5	45.2

4.0.0 Electronics & Software

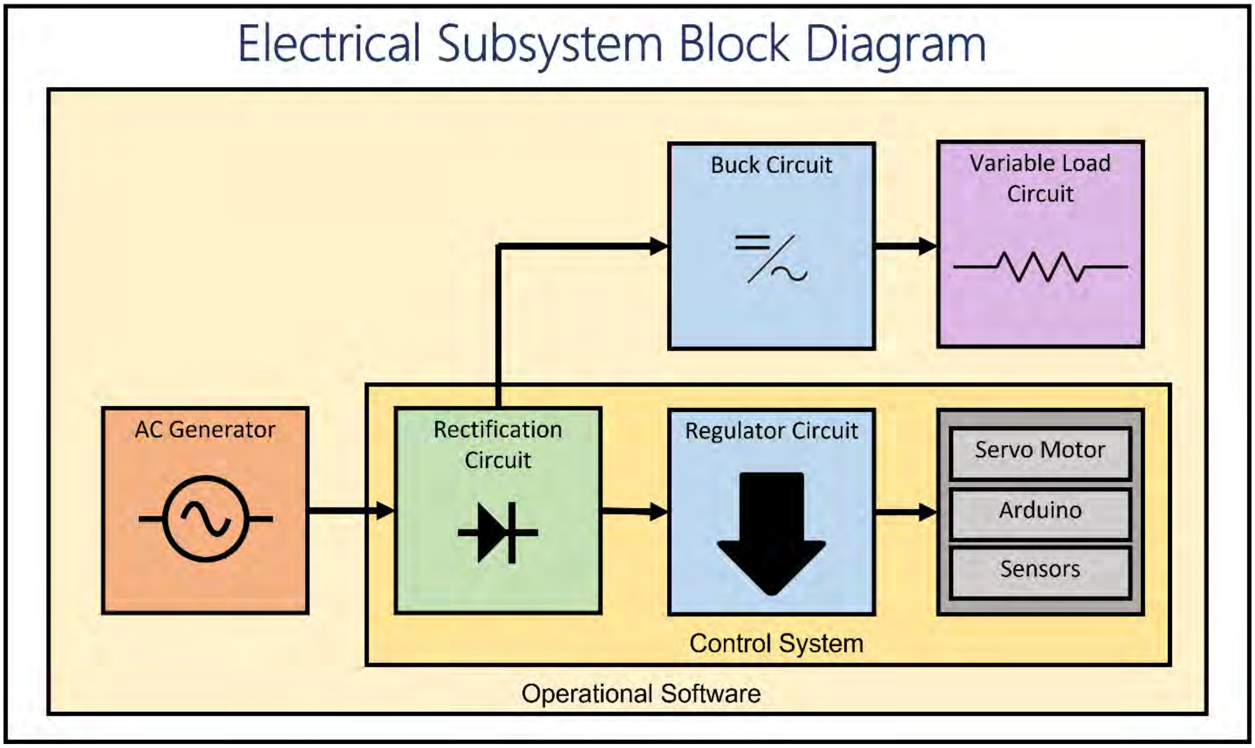

Figure 4.1: Electrical System Block Diagram

The electrical subsystem within the turbine optimizes power production and monitors turbine conditions for safe and efficient operation. The subsystem has been completely redesigned from previous competitions. It has been broken down into three key blocks: the Control System (blue box in Figure 4.2), the Safety Buck Circuit (green box in Figure 4.2), and finally the Variable Load Block (red box Figure 4.2). The operational software controls the full electrical subsystem, and it enables fluid communication between the three blocks. In addition, there are two critical power SPDT (Single Pole Double Throw) relays (black and yellow box in Figure 4.2) utilized in the shutdown, startup, and optimization tasks. The physical power directory relays can be found in Figure 4.3. Due to ongoing semiconductor integrated circuit [IC] shortages, all designs have taken market inventory into consideration.

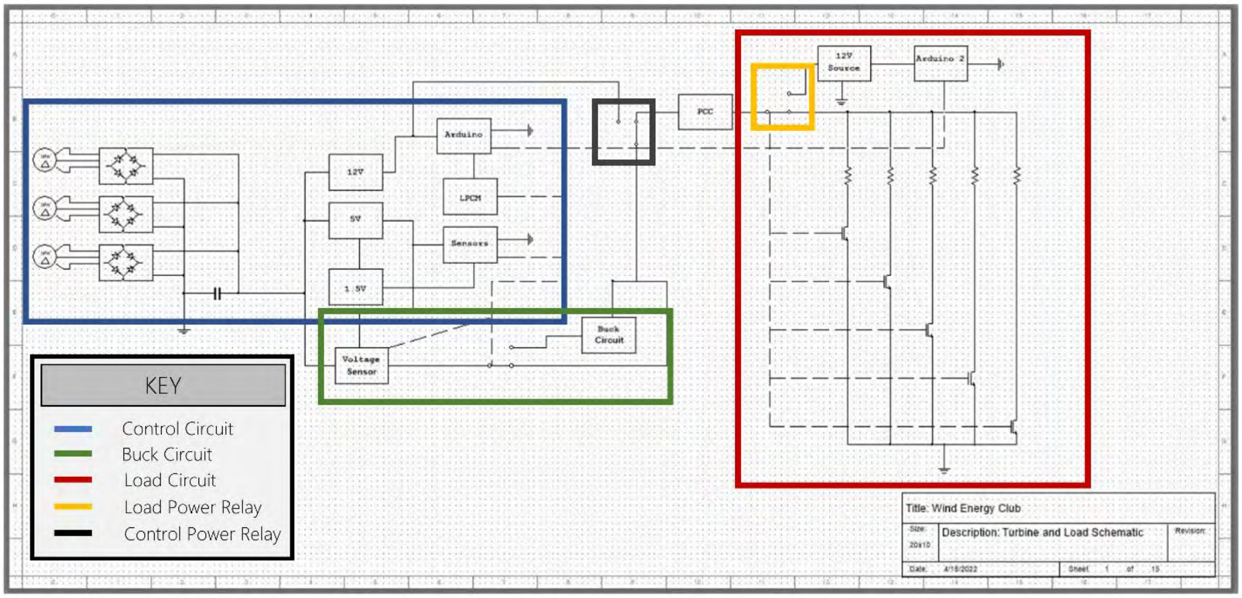

Figure 4.2: Electrical System Generalized Schematic

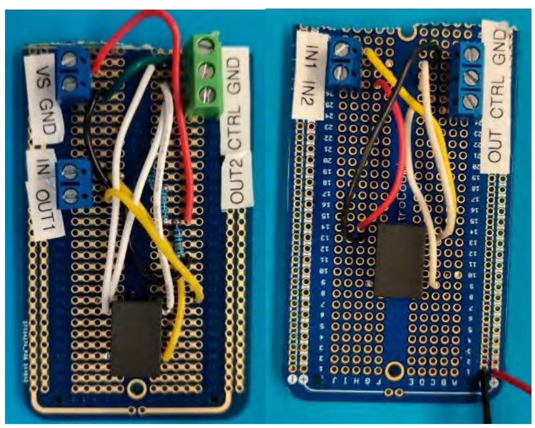

Figure 4.3: Control Power Relay on Left, Load Power Relay on Right

4.1.0 Control States & Safety Tasks

The turbine operates in five active states: Start-Up, Optimization Region I, Optimization Region II, Abnormal Override, and finally the Emergency Shutdown. At all times, the load Arduino is always powered by an off-the-shelf power supply that converts US standard 120V 60Hz AC power to 12V DC power. The turbine is under "Normal Operational Conditions" when it is in Optimization Region I, or Optimization Region II. An overview of the control states can be found in Figure 4.6.

4.1.1 Start-Up

When the turbine activates, it will enter the Start-Up state. The Load and Control Power relays will be set in their default state, so that the system is receiving power from a 12V DC source in the load. This power will be utilized to power the turbine side Arduino which in turn powers the two LPCMs (Linear Pitch Control Motor). In the start-up state, only the voltage sensor, accelerometer, and LPCM will be powered. All other sensors will not be active. The control Arduino will signal the LPCMs to pitch the turbine blade into the start-up blade position (9°), and the load Arduino will adjust the variable load to the highest impedance, 150Ω. The highest load impedance will place the lowest rotational resistance on the turbine.

4.1.2 Optimization Region I

Once the voltage sensor detects steady voltages exceeding 6V, it will transition into Optimization Region I. The Control and Load power directory relays switch the current paths so that the generator is now

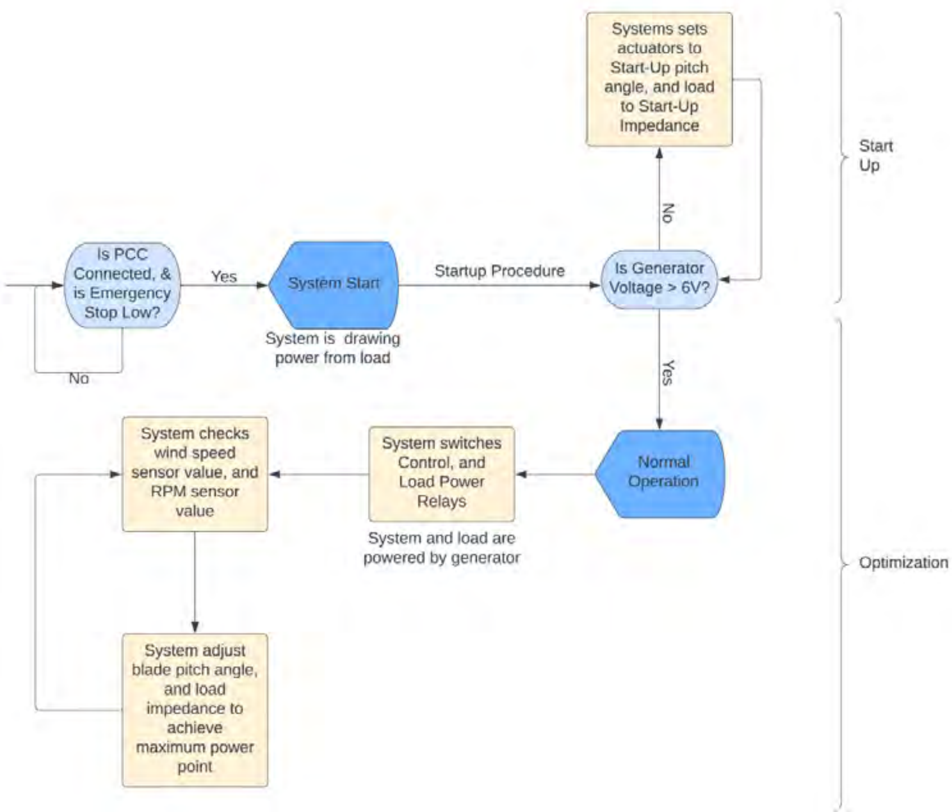

Figure 4.4: Start-Up and Normal Operation

powering the entire turbine system. All sensors are now active and powered. The turbine is now under Normal Operational Conditions. Figure 4.4 Illustrates the turbine's functionality under start-up and normal operation.

In Optimization Region I, the system will run a loop reviewing anemometer wind speed readings, and RPM values. Based on these two readings, the system will reference a library of data sets to determine the most optimal blade pitch angle and load impedance for maximum power. After adjusting the LSM, and load impedance, the turbine will return to the start of the loop.

4.1.4 Optimization Region II

If the voltage sensor detects values exceeding 45V, the turbine will enter Optimization Region II. In addition to the functions of Optimization Region I, The SPDT relay within the safety buck block will switch and direct power through the Buck circuit preventing voltage across the PCC from exceeding 45V. More details on the Buck circuit can be found in section 4.3.0.

4.1.5 Abnormal Override

If the voltage sensor detects values exceeding 60V, the turbine will no longer be categorized under Normal Operational Conditions; the turbine will enter the Abnormal Override state. Since the buck circuit is rated to withstand 63V, exceeding this threshold could cause catastrophic failure of the power system. To avoid this situation, the system will override all optimization tasks, and it will signal the turbine blades to incrementally pitch out of the wind. This process will continue until the voltage sensor detects generator voltage values below 60V.

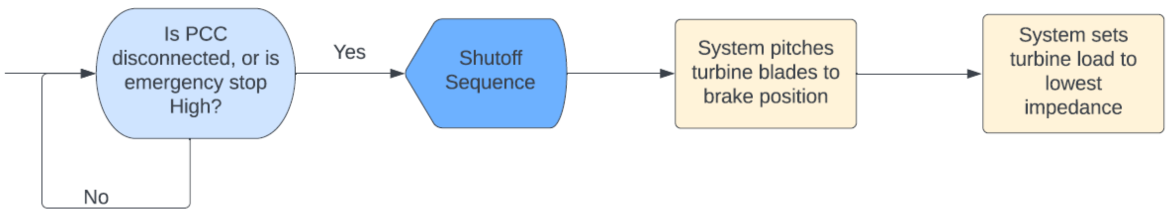

Figure 4.5: Shutdown Sequence

4.1.6 Shutdown Sequence

If the load is disconnected from the turbine or the emergency stop button is depressed, the turbine will enter the Emergency Shutdown state. To stop the turbine, the control Arduino will feather the turbine blades completely into the wind. This will induce a reverse torque quickly slowing the turbine to a stop. The load Arduino will set the load impedance to the lowest value, 10Ω. This will place the highest rotational resistance on the generator. An overview of the Shutdown Sequence can be found in Figure 4.5.

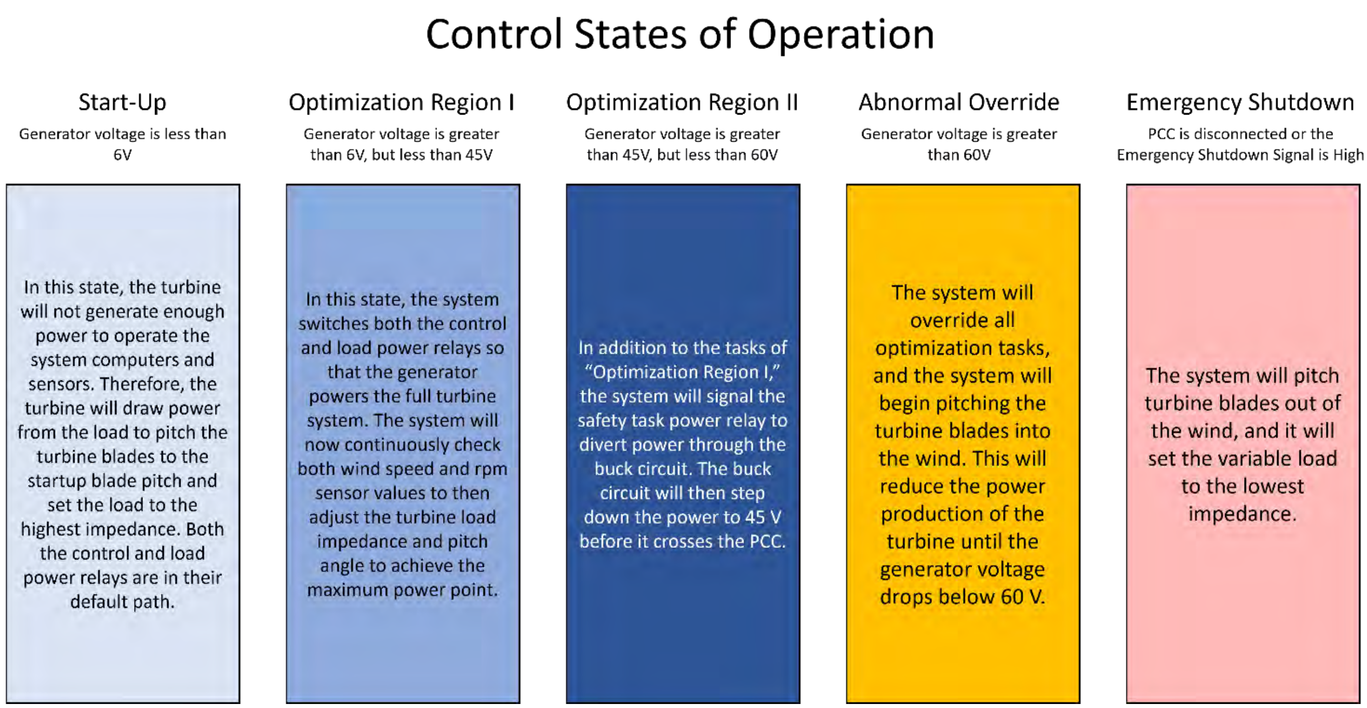

Figure 4.6: Control States of Operation

4.2.0 Control Circuit

The Control Circuit receives an AC signal with nine phases from the turbine generator. A rectification circuit including nine Schottky Bridge Rectifiers is used to convert the input signal to DC Power. An inductor-capacitor filter is also implemented to smooth out any ripples within the DC signal. Most of the rectified power will move across the PCC to power the load, but some of it will move through the regulation circuit to power system sensors and computers.

A series of switching regulation circuits are implemented to efficiently step-down the turbine's rectified power to 12V, 5V, and 1.5V Outputs. The 12V output is solely employed to power the control-side Arduino Uno Microcontroller during the "Optimization I", "Optimization II", and "Abnormal Override" states*. The 5V output will power the turbine anemometer, RPM sensor, accelerometer, Current/Voltage Sensor. Originally the team had planned to use the 1.5V output to power a particular IR sensor to be employed as an RPM sensor; however, through testing, the team had determined the 1.5V IR sensor to have a limited refresh rate that degraded accuracy at high RPMs. Therefore, the team switched to another more accurate IR sensor that draws 5V. The control circuit PCB can be found in Figure 4.7.

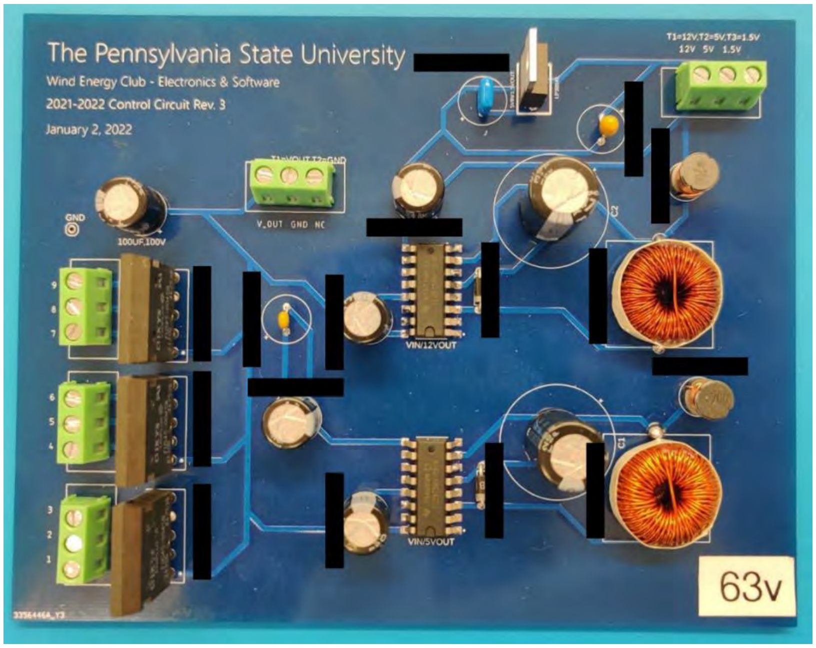

Figure 4.7: Control Circuit

4.3.0 Safety Buck System

Competition constraints limit the voltage across the PCC from exceeding 48V. In prior years, the team would pitch turbine blades to a more inefficient position to reduce overall power output but keep the generator voltage below 48V. The purpose of the new Safety Buck System is to provide a much more efficient method of stepping down voltage while conserving power by increasing current output. The Buck Circuit is configured to limit the voltage across the PCC from exceeding 45V. A 3V buffer was introduced to prevent transient conditions where the voltage across the PCC exceeds 48V. A voltage sensor has been implemented to determine the amplitude of the rectified generator voltage. In the default state, power produced by the generator is sent directly across the PCC. If the voltage sensor value exceeds 45V DC, an SPDT relay will divert the power through the buck circuit. Figure 4.8 illustrated below provides an overview of this process.

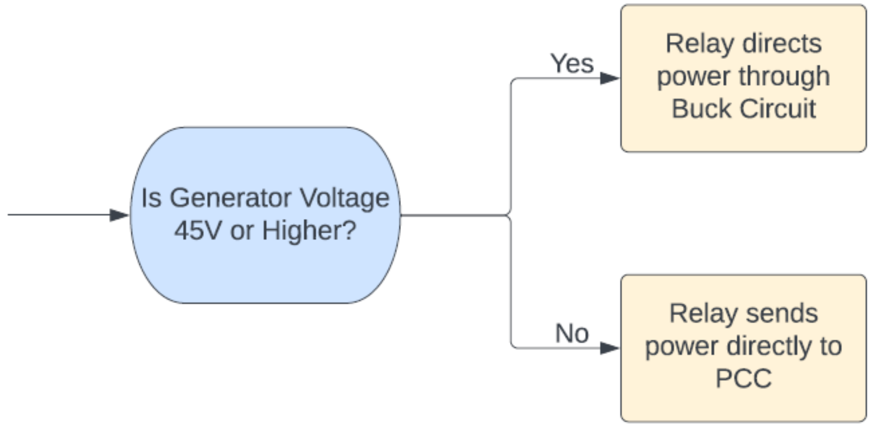

Figure 4.8: Buck Circuit Power Flow Diagram

The buck circuit will step down input power to 45V, and then the circuit will send this output power to the PCC. The buck circuit runs at 80-90% efficiency, so power bypasses the circuit by default; however, if voltage regulation is needed, the buck stage is an efficient means of safely limiting voltage below the competition threshold at the PCC. A PCB of the Buck Circuit can be found in Figure 4.9.

Figure 4.9: Buck Circuit

4.4.0 Variable Load System

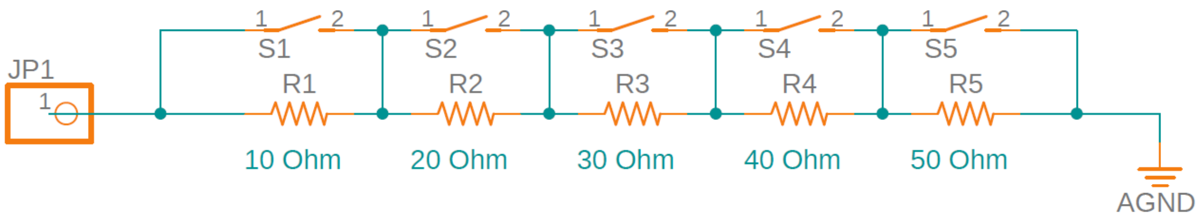

Figure 4.10: Load Schematic

The variable load system is configured to vary the turbine load from 0Ω to 150Ω at increments of 10Ω. It is composed around five power resistors in series that are rated to 100W. Switches controlled by the load Arduino are used to short resistance paths to construct the load impedance. When all switches are off, power will flow through all the resistors for a total resistance of 150Ω. When all the switches are on, no power will flow through the resistors, so the total resistance will be 0Ω. A schematic of the load circuit can be found in Figure 4.10. A schematic of the load circuit can be found in Figure 4.10.

4.5.0 Software

Software written for the control and load circuit Arduinos allow the team's turbine to perform optimally and efficiently. The control software interfaces with the RPM, Wind, and Voltage sensor to calculate an optimal pitch angle and resistance value. The control and load Arduino communicate with each other via the TX and RX ports of the Arduinos. This communication is valuable because data such as RPM, wind speed, and current pitch angle can be viewed by the load Arduino to calculate a resistance value.

The RPM sensor is an IR Sensor that produces a 5V signal when its threshold lighting value is reached. This signal is wired into the Arduino's interrupt timer pin and is activated on the falling edge. An RPM can then be calculated using constants associated with the Arduino Uno and the interrupt timer. The voltage sensor takes a reading of a voltage divider wired into an analog pin of the Arduino. The resistors chosen for the voltage divider allow the maximum range of voltage (60V) to be stepped down to 5V. The 10-bit digital-to-analog converter allows a resolution of ~0.06 V per step giving the Arduino enough clarity to make decisions with the parameter. The remaining wind sensor, current sensor, and accelerometer are off-the-shelf components requiring standard interfacing with software.

To act as a safety mechanism for this year's foundation challenge, an accelerometer was added to monitor the turbine's position and tilt. The function of this is to pitch the blades of the turbine slightly into the wind if the accelerometer detects an angle on the z-axis. This feature allows the team to remain in the testing portion of the competition if a topple would otherwise occur. The amount of angle to pitch into the wind considers the current wind speed and how much topple has already occurred.

5.0.0 Turbine Testing

5.1.0 Power Curve Performance

Over the course of in-house wind tunnel testing, the team was able to collect comprehensive performance data to begin forming a power curve for the turbine. RPM, wind speed, voltage, and current data were recorded over a range of pitch angles. Given that the power curve task only concerns wind speeds from 5-11 m/s, the team decided to collect performance data for these wind speeds. The load for the turbine was kept constant at 50 ohms for the sake of comparing data with prior years, but other trials were performed to determine optimal load as shown in Figure 5.1. A calibration was performed while the turbine was in the wind tunnel to match the blades' pitch angles with their corresponding linear servo values in the Arduino controller. For example, a servo value of 99 in the Arduino software will produce a pitch of 8 degrees.

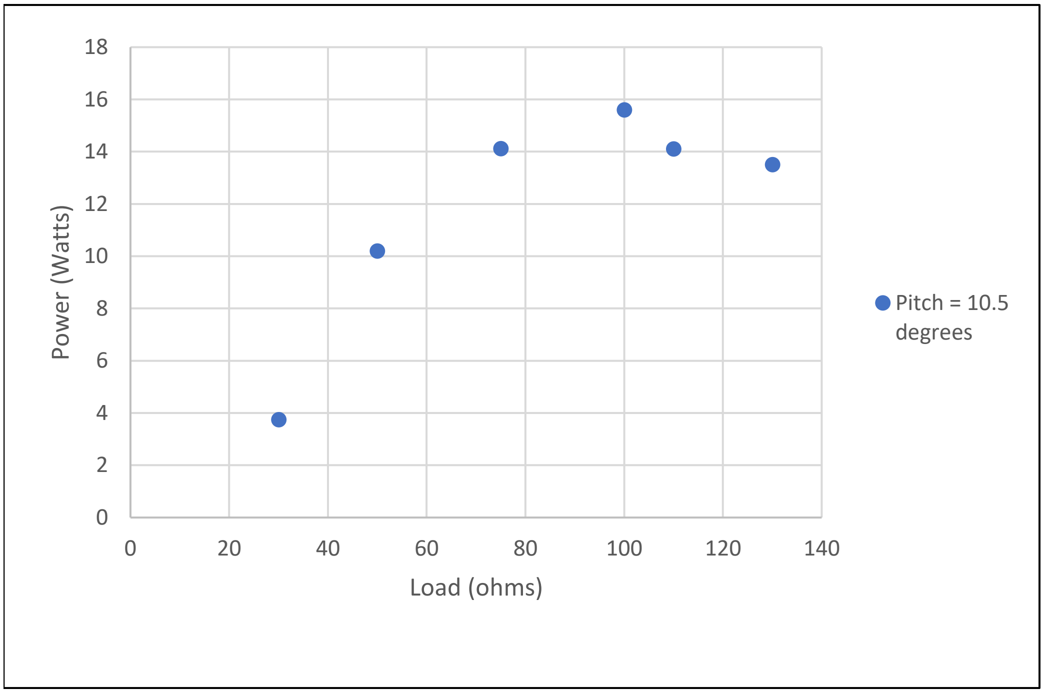

Figure 5.1: Power vs Load at 8m/s

By monitoring the load voltage and current and using the equation P = IV, the power produced by the turbine could be determined at any given instant. Additionally, Equation 2 below was used to find power coefficient values, where A is the rotor disk area, ρ is the air density, P is power, and V is axial wind velocity. This equation also assisted in finding the optimal pitch for each wind speed, as the team varied the pitch to find the angle that produced the maximum C_P at each wind speed from 5-11m/s.

$$C_P = \frac{P}{0.5 * \rho * A * V^3} \tag{2}$$

Furthermore, RPM, Ω, and V were used to find Tip Speed Ratio λ using Equation 3 below.

$$\lambda = \text{RPM} * \frac{\pi}{30} * \frac{\text{R}}{\text{V}} = \frac{\Omega \text{R}}{\text{V}} \tag{3}$$

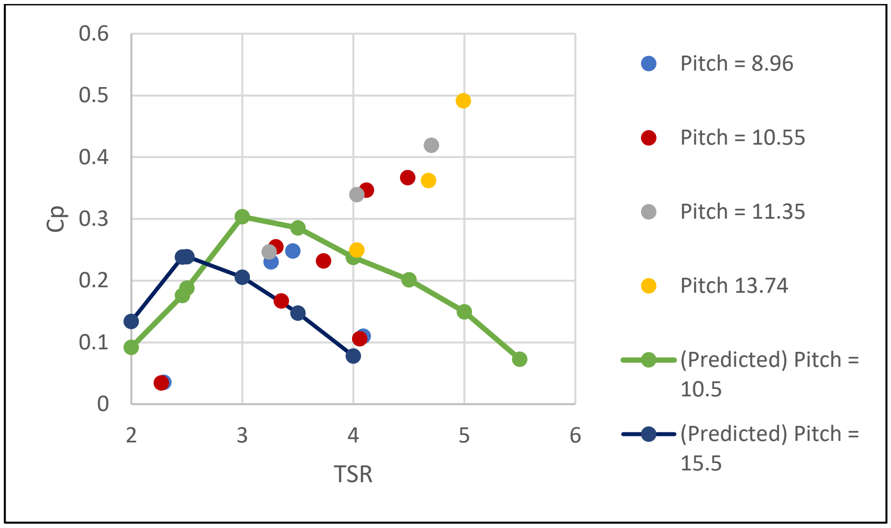

Figure 5.2: Cp vs TSR

With TSR and C_P, these values were plotted for a number of pitch angles shown above in Figure 5.2. However, the simulation and experimental data do not agree at higher tip speed ratios, but the experimental data at lower tip speed ratios is more reasonable. Each measured curve was expected to look similar in shape to those of the predicted curves generated from XTURB also shown in Figure 5.3.

This discrepancy may be explained by blockage in the tunnel. The rotor will produce more thrust at higher tip speed ratios, as shown below in Figure 5.3 produced from XTURB data. Greater thrust causes additional blockage, and this blockage pushes more mass flow through rotor, thereby increasing C_P. At this time, the team does not have a reliable method to correct for tunnel blockage.

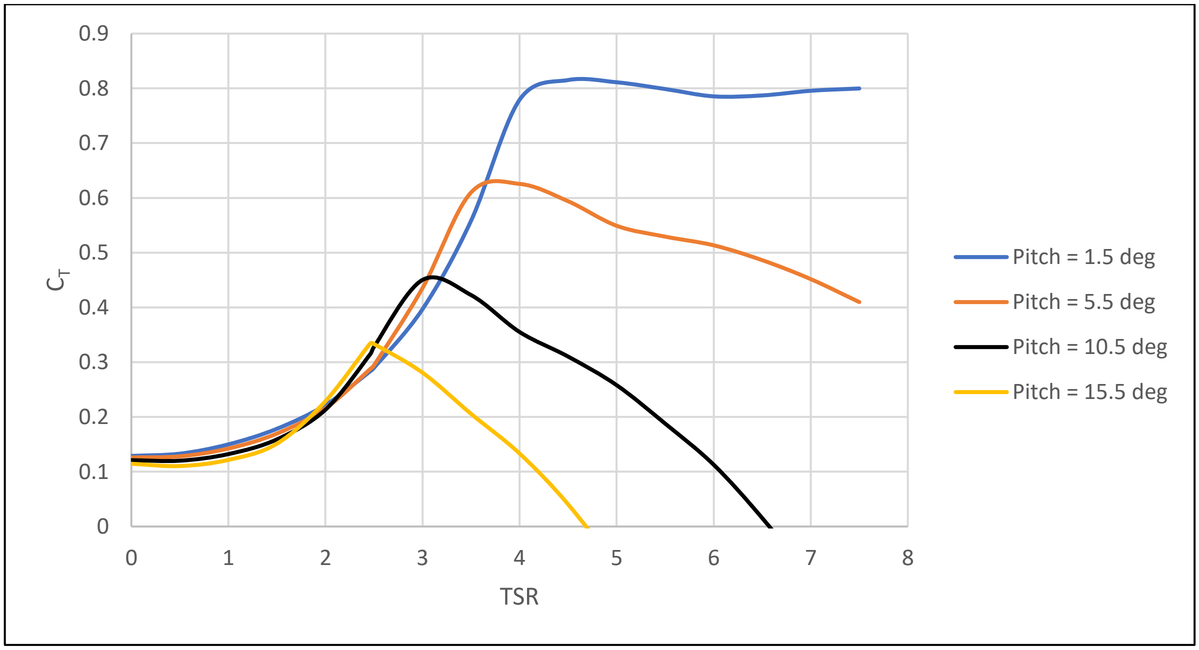

Figure 5.3: Predicted C_T vs TSR

5.2.0 Safety & Restart Task

A complete test of the Safety & Restart Task has not yet been completed. Aerodynamic braking of the turbine has been tested for a variety of windspeeds with success. Extensive experimentation of this task will occur after Technical Design Report submission.

5.3.0 Durability Task

During the first round of wind tunnel testing, the turbine experienced wind speeds of up to 25 m/s for more than five minutes without incurring structural damage. This test was only meant as a shake-down test to ensure the turbine operated as expected. In this test run, the pitch was set to zero degrees, load was kept constant at 20 ohms, and the velocity of the wind tunnel was gradually increased from 2 m/s to 25 m/s while the turbine was closely monitored. Figure 5.4 below shows the results from this test in a Power vs Wind Speed graph. The results are positive for the turbines safety, so the team feels confident in the turbine's ability to perform well in the Durability Task, at least from a power-production perspective. From a structural perspective, the foundation was designed to withstand 50% over the weight and thrust of the turbine.

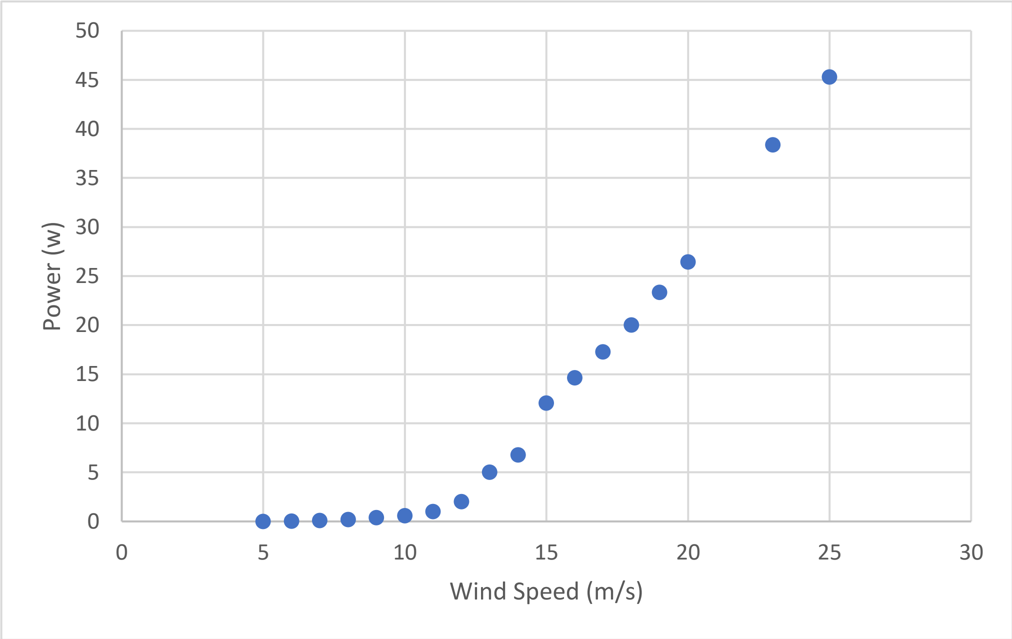

Figure 5.4: Power vs Wind Speed at 20 ohms & Pitch = 0 degrees

5.4.0 Commissioning Checklist

With the addition of a foundation component, the installation and commission of the turbine into the wind tunnel became more complex. To facilitate quick and successful commissioning of our turbine a checklist such as this one becomes more important this year than ever before.

Task	Completed (Double Checked)
Aerodynamics Team	
Assembly of Blades and Pitch Mechanism	

Ensure proper installation of blades	
Test connections of linear servos before installation to nacelle	
Calibrate linear servos, adjust pitch angle formula if necessary	
Attach tailfin at back of nacelle	
Generator	
Assembly of Generator	
Use rotor spacers to properly space stages during installation onto shaft	
Ensure stages are arranged properly such that they fit into slots of nacelle	
Test rotation of generator stages and look for visual or audio irregularities	
Check that collars and bearings are in their proper place	
Ensure all chords are properly fed through tower, and connection to foundation is prepared	
Foundation	
Installation of Foundation	
Assemble foundation, ensure a seal is created, connections are threaded, and all external tools are functional	
Insert foundation into simulation tank, allowing it to sink under its own weight and realigning it before proceeding	
Whilst ensuring proper alignment, vacuum out air and water, allowing the caisson to sink, until sandy water is seen in the reservoir	
Disconnect vacuum, ensure safety of chords	
Insert simulation tank into wind tunnel	
Attach stub, connect electrical components, and install prepared turbine tower	
Electrical & Software	
Assembly of Electrical Box	
Ensure all connections are secure	
Test and ensure calibration of all systems and sensors: generator, pitch mechanism, load and buck circuits, Arduino controlling all sensors	
Connect entire system to PCC	
Initialize all systems for testing	

5.5.0 Conclusion

Every year, the Collegiate Wind Competition designs a challenge for turbines that teams and industry alike seek to overcome. With the challenge of the 2022 CWC being offshore wind, every aspect of the Pennsylvania State University team learned what challenges come with moving from the land to the sea. The PSU 2022 team has overcome these challenges by playing off our strengths and understanding our weaknesses. One of the strongest parts of our team this year was the Electronics & Software team that managed to overhaul the entire electrical system from last year, and still manage to incorporate brand new ideas suck as a buck circuit, RPM sensors, and anemometers. The Aerodynamics team overcame the obstacle of pitching by building a complex mechanism using linear servos that are far more accurate and have greater range of pitch. The Generator team investigated active stage variation, which is a derivation from how actual turbines manage output. Finally the new Foundation team research, designed, and modeled a suction caisson foundation that will allow the team ample time for instillation during the competition.

Appendix A. Overall Design Choices

Team	New	Revised/Improved	Identical to 2021 or earlier
Aero	Blade pitch mechanism	Blade 3D prints & material	Blade chord and twist distr.
Generator	Active stage variation	Stage spacing	Rotors and stators
	Rotor spacing mechanism		
Electronics & Software	Variable Load System and Safety Buck System	Control System (Rectification and Regulation),	N/A
	Start up, Shutdown, and Optimization States	Voltage Sensor	
	RPM Sensor, Anemometer, Accelerometer, Current Sensor		
Foundation	Suction caisson	N/A	N/A

References

[1] Schmitz, Sven. *Aerodynamics of Wind Turbines: A Physical Basis for Analysis and Design*. John Wiley & Sons, 2020.

[2] Schmitz, Sven. XTurb-PSU. https://www.rotoraero.psu.edu/xturb-psu/

[3] Folmar, Eric T. (2022). *Effectiveness of Active Stage Variation in an Axial Flux Permanent Magnet Generator for Small Wind Turbine Applications.* The Pennsylvania State University Schreyer Honors College, 2022.

[4] The Offshore Wind Accelerator. (2019) *Suction Installed Caisson Foundations for Offshore Wind: Design Guidelines* (Issue 1.0). The Offshore Wind Accelerator. https://prod-drupal-files.storage.googleapis.com/documents/resource/public/owa-suction-caisson-design-guidelines-report.pdf

[5] Zhu, F.Y. (2018). Suction caisson foundations for offshore wind energy installations in layered soils.